SUPPLEMENTARY DATA

Structures of Rhodopsin Kinase in Different Ligand States Reveal Key Elements Involved in G Protein-Coupled Receptor Kinase Activation

Puja Singh, Benlian Wang, Tadao Maeda, Krzysztof Palczewski, and John J.G. Tesmer

SUPPLEMENTARY METHODS

Cloning of $GRK1_{535}$-His_6. The pFastBac Dual vector (Invitrogen) was re-engineered to introduce a hexa-histidine tag and a stop codon following the *SalI* site downstream of the polyhedrin promoter. PCR fragment encoding residues 1-535 of bovine GRK1 were ligated into the *BamHI*/*SalI* sites. Recombinant protein produced from this template ($GRK1_{535}$-His_6) contains exogenous Val and Asp residues (*SalI* sequence) preceding the non-cleavable hexa-histidine tag at the C-terminus.

Site-directed Mutagenesis. The dimer-interface (D164A, L166K, W531A, D164A/L166K, D164A/W531A, L166K/W531A) and the N-terminal mutants (S5A, S5D, T8A, T8E, T8D) of bovine GRK1 were generated in pFastBac HTB vector (Invitrogen) using QuikChange Mutagenesis Kit (Stratagene). Following digestion with TEV protease, wild-type GRK1 and mutants contained five exogenous residues (Gly-Ala-Met-Gly-Ser) at the N-terminus.

Crystallization. $GRK1_{535}$-His_6 pool A (7-12 mg/ml) was used for crystallization by the hanging drop vapor diffusion method mixing 0.8-1.0 μL protein solution in a 1:1 ratio with the well solution. Six crystal forms were characterized (Supplementary Fig. S11). Crystals grown in the presence of nucleotides contained protein pre-mixed with a final concentration of 2 mM $MgCl_2$ and either 4 mM ATP or ADP, pH 7.5. All were grown at 4˚C except for crystal form IV. Crystals of GRK1·$(Mg^{2+})_2$·ATP appeared under two different conditions. Well solutions consisted of 11% PEG 6000, 200 mM NaCl, 5% glycerol, 100 mM Na-tartarate, pH 4.35 (crystal form I) and 12% PEG 3350, 200 mM NaCl, 5% glycerol, 100 mM Na-citrate, pH 4.3 (crystal form II). Cryoprotectants consisted of the respective well solutions with 20 mM HEPES, pH 7.5, 2 mM DTT, 25% glycerol, 4 mM ATP, pH 7.5, and 2 mM $MgCl_2$.

Apo-GRK1 grew as hexagonal plates (crystal form III) using a well solution containing 11% PEG 3350, 200 mM NaCl and 100 mM MES, pH 6.4, and the cryoprotectant consisted of 20 mM HEPES, pH 7.5, 2 mM DTT, 11% PEG 3350, 200 mM NaCl, 100 mM MES and 25% glycerol.

Crystals of GRK1·$(Mg^{2+})_2$·ADP were grown under three different conditions (crystal forms IV-VI). Crystal Form IV grew using well solution containing 22% PEG 6000, 1 M NaCl, 5% glycerol and 100 mM MES, pH 6.25. The cryoprotectant contained 20 mM HEPES, pH 7.5, 2 mM DTT, 4 mM ADP, pH 7.5, 2 mM $MgCl_2$, 24% PEG 6000, 1.2 M NaCl, 100 mM MES, pH 6.25, and 25% glycerol. Crystal Form V grew using well solution containing 15% PEG 8000, 900 mM NaCl, 100 mM MES, pH 6.25, and 5% glycerol. The cryoprotectant consisted of 20 mM HEPES, pH 7.5, 2 mM DTT, 4 mM ADP pH 7.5, 2 mM $MgCl_2$, 17% PEG 8000, 1.3 M NaCl, 100 mM MES, pH 6.25, and 25% glycerol. Crystal Form VI grew using well solution containing 15% PEG 8000, 800 mM NaBr, 100 mM MES, pH 6.25, and 5% glycerol. The cryoprotectant consisted of 20 mM HEPES, pH 7.5, 2 mM DTT, 4 mM ADP, pH 7.5, 2 mM $MgCl_2$, 17% PEG 8000, 1.0 M NaBr, 100 mM MES, pH 6.25, and 25% glycerol. Crystal forms IV and V were

harvested in the presence of 10 mM peptides derived from the C-terminus of Rho, but densities corresponding to these peptides were not observed in these structures.

Purification of GRK1 from Bovine Retina. Native GRK1 was purified from bovine retina as published previously with some modifications (1). Briefly, 50 frozen bovine retinas were homogenized in 75 ml modified ROS buffer (20 mM Bis-Tris propane (BTP), pH 7.5, with 30 mM NaCl, 60 mM KCl, 1 mM $MgCl_2$, 5 mM KF, 1 mM dithiothreitol, 0.1 mM n-dodecyl-ß-D-maltoside, and 1 mM benzamidine) with 1 mM EDTA under safe light (Kodak No.1 film) and centrifuged at 25,900 *g* at 4 °C for 45 min. The supernatant was dialyzed against 10 mM BTP, pH 7.5, with 1 mM benzamidine and 5 mM KF. The dialyzed solution was applied to a 2.5 x 10-cm DE-52 column (Whatman) equilibrated with the dialysis buffer. The column was washed until the absorbance at 280 nm dropped below 0.01 OD, and bound proteins were eluted with modified ROS buffer. Extracts containing the major kinase activity were collected and loaded to CNBr-activated Sepharose CL-4B beads coupled to recoverin (2.5 x 5 cm) and equilibrated with modified ROS buffer containing 2 mM $CaCl_2$. GRK1 was eluted from recoverin-coupled CNBr-activated Sepharose with modified ROS buffer containing 5 mM EGTA. Collected fractions were assayed for kinase activity as described below. The major fractions with GRK1 activity were concentrated with Centricon 30 (Millipore) and analyzed by SDS-PAGE (Supplementary Fig. S10, Table S3).

ROS and Synuclein Phosphorylation. ROS phosphorylation assays were carried out as described by Pronin et al (2) using urea-stripped ROS (uROS) as a substrate. Similar assays were performed using 2.5 μM α-synuclein as a substrate. Reactions were quenched by addition of SDS-loading buffer. The dried gel was used to expose a phosphorimager screen that was scanned with a Typhoon 9410 Imager (Amersham).

Recoverin Binding Assay. 50 μg $GRK1_{535}$-His_6 from Pools A, B and C were incubated with 30 μl CNBr-activated Sepharose CL-4B beads coupled to nonacylated-recoverin for one hr at 4 °C. The assay conditions were similar to recoverin affinity purification of GRK1 (1). Binding efficiency was monitored by SDS-PAGE.

Size Exclusion Chromatography and Sedimentation Equilibrium. To determine the aggregation state of soluble GRK1, 75 μM $GRK1_{535}$-His_6 (Pool A) was loaded onto two tandem Superdex 200 HR 10/30 preparative columns (Pharmacia) pre-equilibrated with 20 mM Na-HEPES, pH 7.5, 100 mM NaCl and 1 mM DTT at a flow rate of 0.3 ml/min. Sedimentation equilibrium analysis was carried out in a Beckman Optima XL-1 analytical ultracentrifuge as described for GRK6 (3). $GRK1_{535}$-His_6 (Pool A) post-size exclusion chromatography was used for the analysis at four different rotor speeds (7,000, 10,000, 15,000 and 25,000 rpm).

Structure Figures. Rendering of the molecular structure of GRK1 was performed using PyMOL (http://pymol.sourceforge.net/).

SUPPLEMENTARY TABLES

Table S1. Data Collection and refinement statistics

Crystal Form (PDB)	**I (3C4W)**	**II (3C4X)**	**III (3C4Y)**	**IV (3C4Z)**	**V (3C50)**	**VI (3C51)**
Ligand	$(Mg^{2+})_{1\text{ or }2}$·ATP	$(Mg^{2+})_{1\text{ or }2}$·ATP	Apo	$(Mg^{2+})_2$·ADP	$(Mg^{2+})_2$·ADP	$(Mg^{2+})_2$·ADP
Data collection						
Space group	C2	$P2_12_12_1$	$P3_221$	C2	$P2_12_12_1$	$P2_12_12_1$
Unit cell						
a, b, c (Å)	202.9, 55.0, 122.7	54.1, 95.1, 234.8	123.3, 123.3, 192.5	65.5, 82.9, 107.1	65.5, 122.3, 174.1	58.6, 92.5, 259.4
α, β, γ (°)	90, 100.8, 90	90, 90, 90	90, 90, 120	90, 93.0, 90	90, 90, 90	90, 90, 90
D_{min} (Å)	2.7	2.9	7.51	1.84	2.60	3.55
R_{sym} [b]	9.6 (64.7) [a]	9.4 (51.6)	8.4 (79.1)	5.5 (49.5)	8.9 (51.2)	9.6 (47.9)
I/σ_I	22.9 (3.1)	13.1 (2.1)	24 (2.7)	35.1 (3.0)	19.8 (2.7)	17.4 (2.2)
Completeness (%)	99.7 (100)	96.2 (94.2)	100 (100)	99.4 (99.2)	99.8 (99.9)	97.6 (94.2)
Redundancy	6.8 (6.6)	3.9 (4.0)	7.2 (7.6)	4.2 (4.2)	5.8 (5.9)	3.6 (3.6)
Refinement						
Resolution (Å)	20 - 2.7	20 - 2.9	20 - 7.51	20 - 1.84	20 - 2.60	20 - 3.55
No. reflections	36,930 (2,668)[c]	26,552 (1,822)	2,230 (156)	49,141 (3,591)	43,677 (3,124)	17,299 (1,184)
R_{work} [d]	19.1 (27.7)	19.2 (29.5)	18.8 (42.8)	19.1 (24.3)	19.0 (27.9)	27.7 (30.8)
R_{free} [e]	24.6 (31.9)	25.6 (35.0)	27.4 (44.4)	21.7 (26.7)	23.8 (32.9)	35.1 (40.2)
R_{final} [f]	19.2 (26.9)	19.3 (28.0)	18.2 (40.0)	19.3 (24.4)	18.9 (26.8)	28.1 (30.3)
Protein atoms	8156	7841	7629	4017	8,057	7637
Non-protein atoms	232	126	0	365	381	63
Wilson B factor (Å^2)	64.2	72.9	ND	30.8	53.0	ND
Average B factor (Å^2)						
Protein atoms	46.9	49.3	191.7	37.5	40.6	137.7
Ligands	36.2	47.0	0	30.7	41.4	133.5
Solvent	36.0	29.2	0	42.2	36.6	0
R.m.s deviations						
Bond length (Å)	.012	.010	.009	.009	.010	.008
Bond angles (°)	1.4	1.2	1.1	1.2	1.2	1.1
Ramachandran plot						
most favored (%)	92.5	90.7	79.5	92.3	90.0	86.4
disallowed (%)	0.0	0.0	0.2	0.0	0.0	0.0

[a] Numbers in parentheses correspond to the highest resolution shell of data; Crystal Form I: 2.8-2.7 Å; Crystal Form II: 3.0-2.9 Å; Crystal Form III: 7.77-7.5 Å; Crystal form IV: 1.91-1.84 Å; Crystal form V: 2.69-2.60 Å; Crystal form VI: 3.68-3.55.

[b] $R_{sym} = \sum_{hkl}\sum_i |I(hkl)_i - I(hkl)|/ \sum_{hkl} I(hkl)_i$, where I(*hkl*) is the mean intensity of *i* reflections after rejections.

[c] Numbers in parentheses correspond to the highest resolution shell of data; Crystal Form I: 2.77-2.7 Å; Crystal Form II: 2.97-2.90 Å; Crystal Form III: 7.68-7.51 Å; Crystal form IV: 1.89-1.84 Å; Crystal form V: 2.67-2.60 Å; Crystal form VI: 3.64-3.55.

[d] $R_{work} = \sum_{hkl}||F_{obs}(hkl)| - |F_{calc}(hkl)||/ \sum_{hkl} |F_{obs}(hkl)|$; no I/σ cutoff was used during refinement.

[e] 5% of reflections were excluded from refinement to calculate R_{free}.

[f] All reflections were used during the last rounds of refinement.

ND = Not determined.

Table S2. Rotation of large lobe relative to small lobe required to achieve an active conformation similar to that of PKA

	PKA_c	PKB_c	PKA_o	PKB_o	GRK1-I	GRK1-II	GRK1-IIIa	GRK1-IIIb	GRK1-IV	GRK1-V	GRK1-VI	GRK2	GRK6
PKA_c	**0**	**4**	**13**	**13**	**14**	**13**	**20**	**12**	**15**	**13**	**15**	**20**	**17**
PKB_c		0	129	29	110	108	130	132	103	107	109	97	120
PKA_o			0	100	20	24	8	20	29	26	24	32	14
PKB_o				0	81	79	101	103	74	78	81	68	91
GRK1-I					0	5	20	27	10	8	8	13	11
GRK1-II						0	22	26	5	3	4	14	12
GRK1-IIIa							0	12	27	23	21	33	10
GRK1-IIIb								0	31	26	23	39	15
GRK1-IV									0	4	7	11	17
GRK1-V										0	3	15	13
GRK1-VI											0	17	11
GRK2												0	24
GRK6													0

The "c" and "o" subscripts refer to the "closed" (catalytic) and "open" conformations of PKA and PKB. PKA_c = PDB code 1L3R; PKA_o = 1CMK; PKB_c = 1O6K; PKB_o = 1MVR. For GRK1 and GRK6, the sequence analyzed corresponds to the "A" chain of their structures. Red numbers are the degrees required to superimpose the kinase large lobe of each of these structures with that of PKA_c. All other values indicate the difference, in degrees, between the rotation axes required to superimpose the large lobes, as determined by the direction cosines of each of the rotation axes. Hence, small values indicate that the rotation axes are similarly oriented, and large values indicate large discrepancies (e.g. 90˚ indicates they are orthogonal). Not all the rotation axes intersect, however. Whereas the GRK rotation axes required to achieve the closed conformation are quite similar and intersect (with the exception of crystal form III, green highlights), those required to close the domains of PKA and PKB are unique. Note that among the GRK1 rotation axes, those of the apo-GRK1 (crystal form III) are the most divergent (yellow highlights). They are most similar to, although significantly different from, each other (blue highlight), indicating not only a large degree of flexibility in apo-GRK1, but also a discrete conformational state. The conformation of the apo-GRK1 domains are most similar to those of GRK6 (2ACX, grey highlights).

Table S3. Purification of GRK1 from retinas

Purification step	Volume (ml)	Protein (mg)	Activity (nmol P_i/min)	Specific activity (nmol P_i/min/mg)
supernatant from 50 retinas	40.0	744.0	0.06	0.3
DEAE cellulose column	12	31	120	4.6
Recoverin-coupling column	3.0	0.10	442	1473

Table S4. Phosphorylation sites identified by LC-MS/MS

Sequence (phosphorylation sites underlined)	$GRK1_{535}$-His_6[†]	Retina GRK1
Acetyl-MDFGSLETVVANSAFIAAR	S5, T8	S5
GSFDASSGPASR	S21	S21
NIQDVGAFSTVK	S488, T489	
NIQDVGAFSTVKGVAFEK		S488, T489

[†] $GRK1_{535}$-His_6 (Pool A) was incubated with 4 mM ATP (pH 7.5) and 2 mM $MgCl_2$ at 4 °C overnight to mimic crystallization conditions. See Fig. 3b and Supplementary Fig. S7.

Table S5. N-terminal sequencing and MS analysis of $GRK1_{535}$-His_6

Sample	N-terminus[†]	Intact mass[‡] (Da)	Expected Mass[‖] (Da)
Pool A	N-terminal acetylated	61,390 and 61,488	61,390
Pool B	Thr^8	60,659 and 60,567	60,568
Pool C	Ala^{17}	59,672	59,665

[†]N-terminal sequence analysis was performed on protein from two different purifications.

[‡]$GRK1_{535}$-His_6 samples (Pool A, B and C) were desalted using Vydac C4 ultramicrospin column (Nest Group) according to the manufacturer's protocol and then reconstituted in 50% acetonitrile-0.1% formic acid. Samples were infused into a QSTAR XL mass spectrometer (Applied Biosystems) via a syringe pump at 0.5 μl/min. The intact protein mass was analyzed by Bayesian protein Reconstruct using Analyst QS 1.1 software. The masses corresponding to the major peaks in each sample are reported.

[‖] Expected masses were calculated based on the primary sequence of $GRK1_{535}$-His_6 after taking into account the N-terminal acetylation (for Pool A) or N-terminal truncations (for Pool B and C).

Figure S1. The GRK1 dimer interface from crystal form I. $GRK1_{535}$-His_6 crystallizes as a dimer using a conserved interface of the RH domain. There is, however, considerable flexibility within the interface, evidenced by the fact that the relative orientation of the dimer subunits differs among the crystal forms. For example, a rotation of ~15° orthogonal to the two-fold axis is needed to align the B chains of crystal forms I and V when their A chains are first superimposed. **Inset**. Close-up of the dimer interface. The terminal subdomains have been colored slate and magenta to represent the two monomers. The side chains of Trp531 and Tyr167 form stacking interactions with their dimer equivalents, and Asp164 forms a hydrogen bond with the backbone of the opposing monomer. The Leu166 and Leu44 side chains also contribute to the hydrophobic core of the interface. Two symmetry-related chloride ions are observed to bridge the dimer interface, where they interact with the side chains of Arg170 and Gln173 from one chain, and a backbone amide from the other.

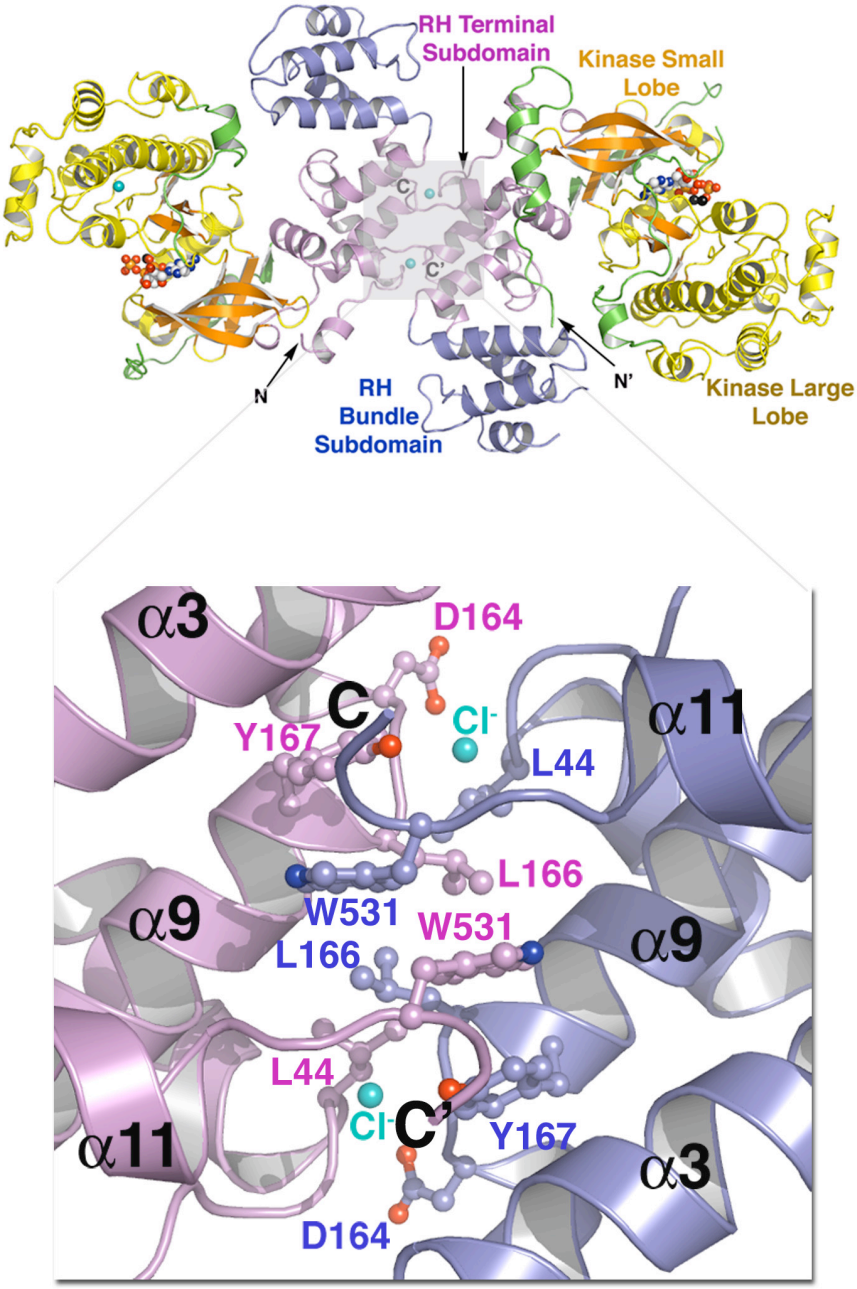

Figure S2. The RH-large lobe interface in GRK1. An interface between the RH bundle subdomain (shown in slate) and the C-terminal extension (green) of the kinase domain (yellow) has now been observed in all three GRK subfamilies. The RH-large lobe interface shown is from the 1.85 Å structure of crystal form IV. Arg458 (αJ helix) forms hydrogen bonds with the backbone of the α4-α5 loop and a salt bridge with Asp100. The side chains shown are conserved in all GRKs except GRK2 and GRK3. The role of this interface is not known, but it could represent a stabilizing interaction for the C-terminal extension of the kinase domain, which begins with the αJ helix.

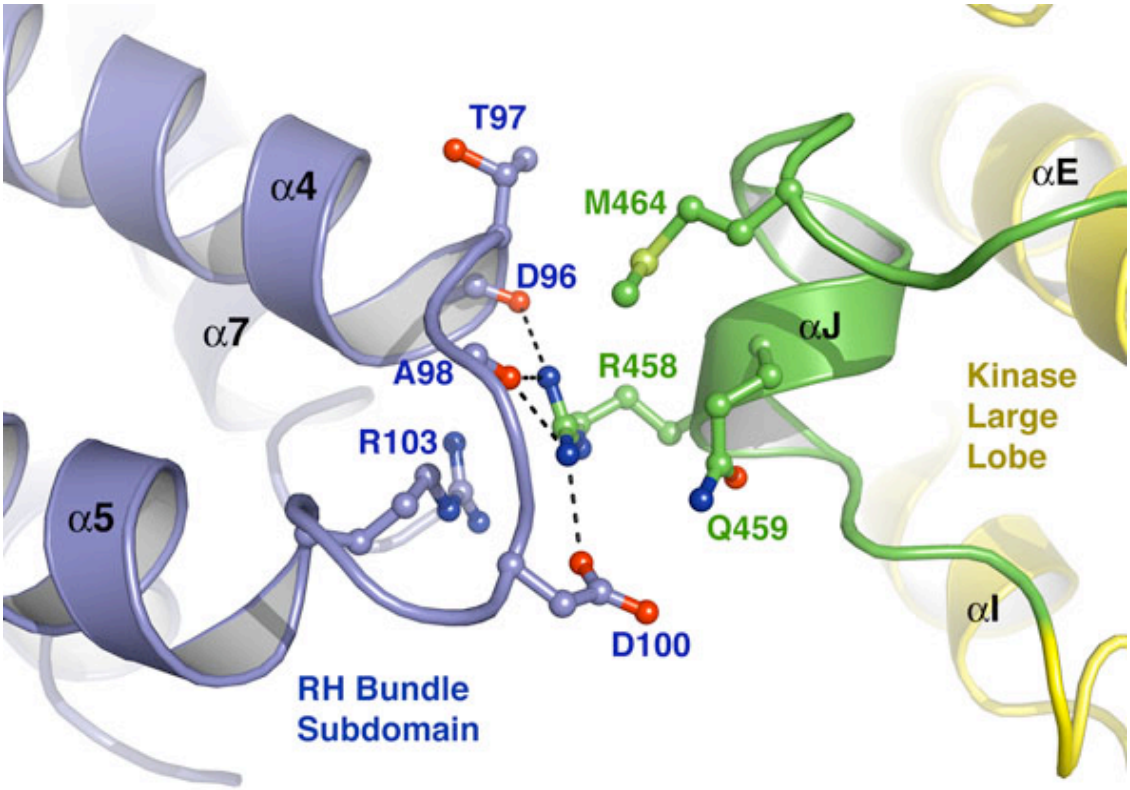

Figure S3. Open and closed states of the GRK1 kinase domain. (a) The small lobe of the transition state PKA complex (grey) was aligned with that of the GRK1·$(Mg^{2+})_2$·ADP (magenta) complex to compare the relative orientations of their large lobes. The brown circle indicates the position of the rotation axis (pointing out of the plane of the figure) around which the large lobe of GRK1 would have to rotate 15˚ counter-clockwise to assume the same conformation as PKA. The insets show the same comparison but with superposition of the large lobes. **(b)** Comparison of the open and closed states of PKA. The view is rotated slightly around a vertical axis from panel (a). A rotation of 13˚ is required to superimpose their large lobes. Note that although the rotation axis points in a similar direction, it is in a distinct location from that in (a). **(c)** Chain A of the apo-GRK1 structure is most similar to the open conformation of PKA. A rotation of 9˚ is required to superimpose their large lobes.

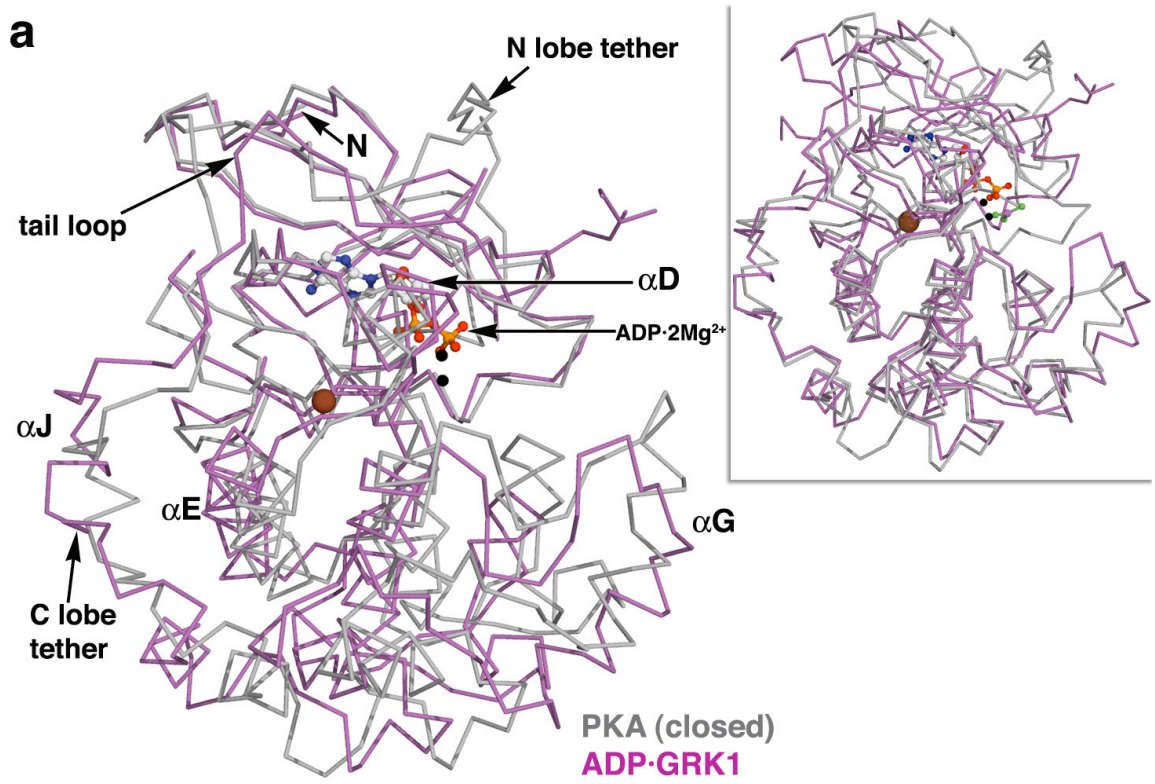

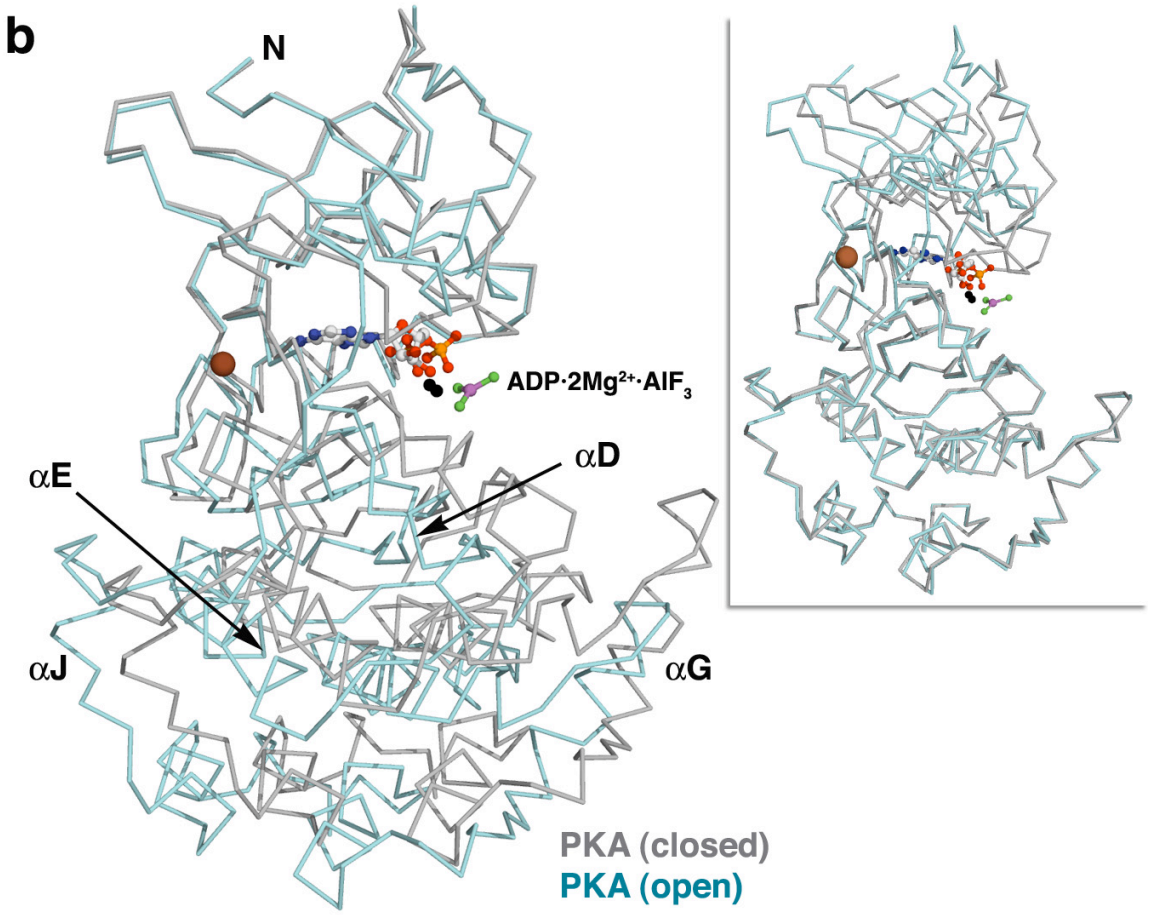
b
N
ADP·2Mg2+·AlF3
αD
αE
αJ
αG
PKA (closed)
PKA (open)

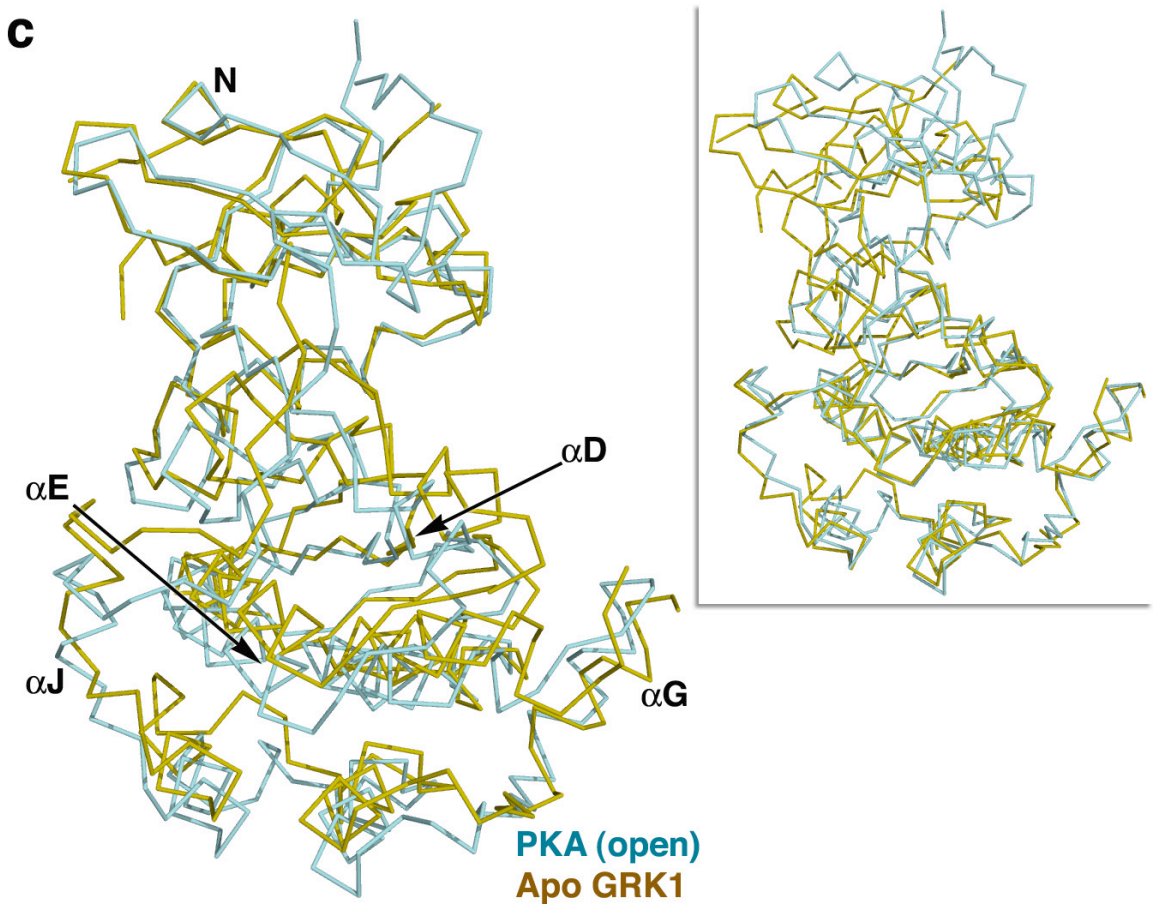
C
N
αD
αE
αJ
αG
PKA (open)
Apo GRK1

Figure S4. Average backbone B factors. The average main chain B factors for crystal form IV and chain B of crystal forms I and V are shown as a plot of the average main chain B factors as a function of residue number, with gaps corresponding to disordered residues. Regions that differ significantly in conformational flexibility have been labeled. The high apparent mobility of the αF-αG loop in crystal form I is due to the fact that the loop is involved in an extensive crystal contact in the other two crystal forms. In GRK2 and GRK6 structures, the analogous loop is likewise poorly ordered. The RH domain of Crystal Form IV has less mobility in the RH domain presumably due to a novel crystal contact involving the bundle subdomain of the RH domain.

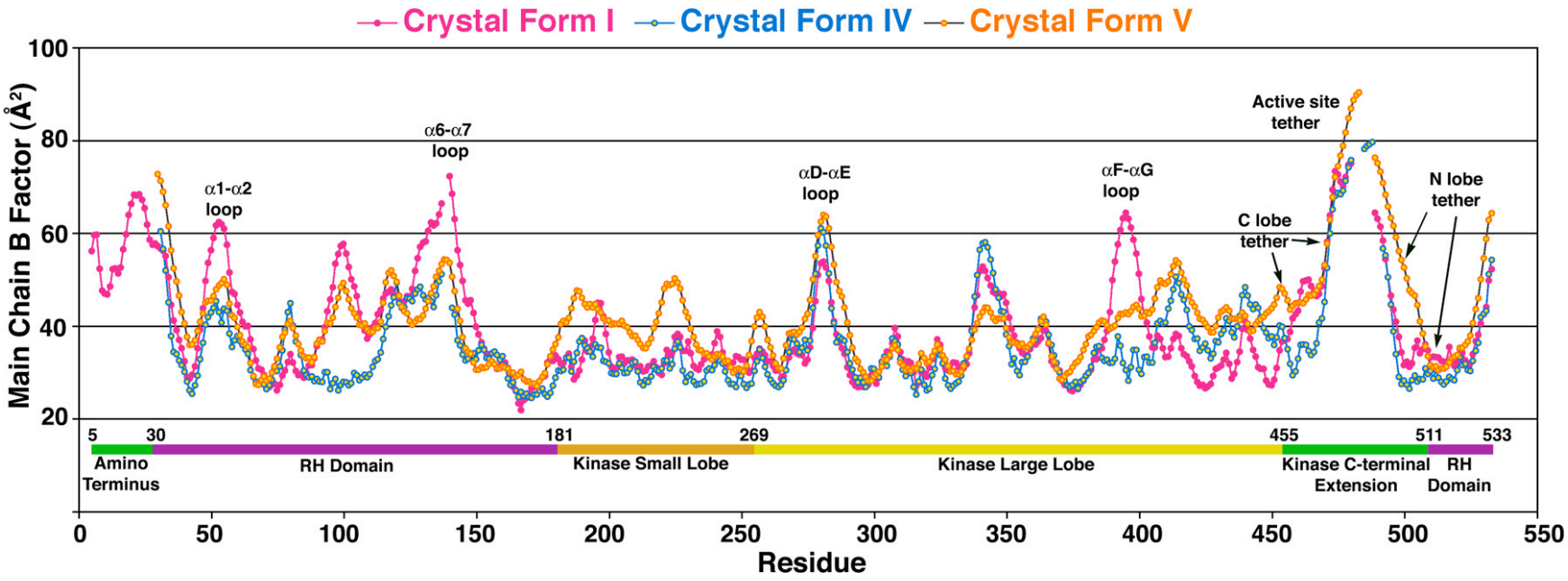

Figure S5. Electron density omit maps. (a) In chain A of crystal form I, the structural Mg^{2+} ion in the active site is displaced by the Nζ atom of Lys497 (green carbons) donated by a crystal contact. As a consequence, the ribose sugar of ATP adopts the C2'-endo as opposed to the C3'-endo conformation observed in the other GRK1 nucleotide complexes. The σ_A-weighted $|F_o|-|F_c|$ omit map is contoured at 4σ, wherein ATP, Mg^{2+} and associated waters were excluded from refinement. **(b)** The extreme N-terminus of GRK1 is observed in chain B of crystal form I. The σ_A-weighted $|F_o|-|F_c|$ omit map is contoured at 3σ, wherein the residues 5-30 (crystal form I, chain B) were excluded from refinement. Strong electron density for the phosphate adduct on Thr8 is evident. For clarity, only the first six residues are shown.

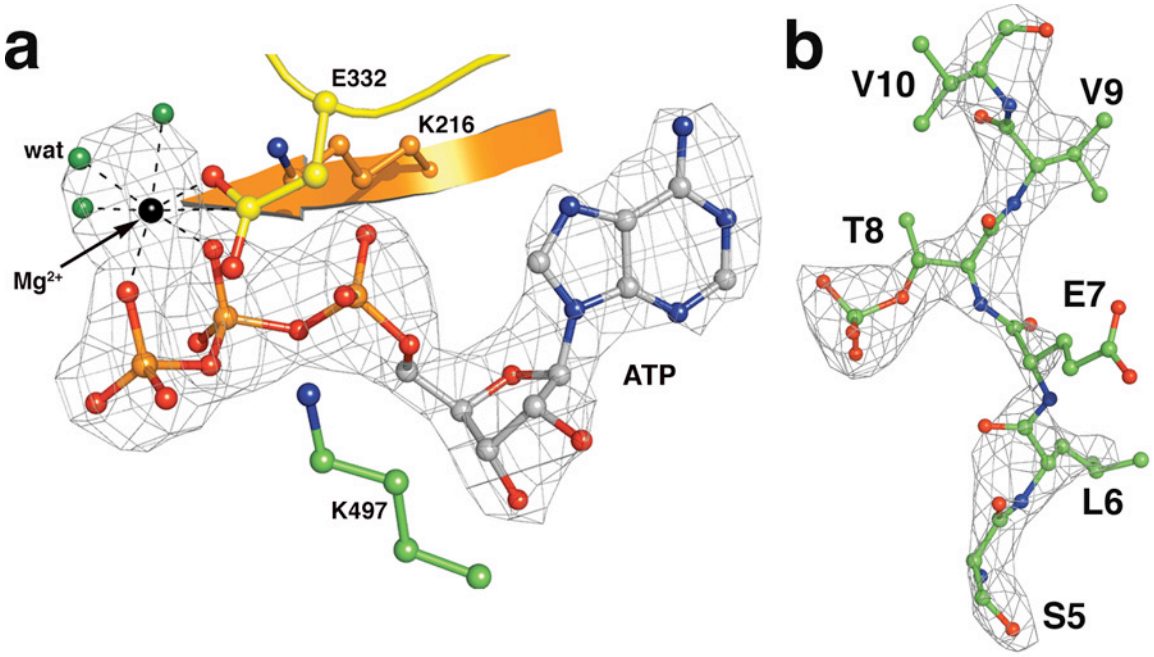

Figure S6. Stabilization of native GRK1 after ATP incubation. (a) Migration of purified, endogenous GRK1 after incubation with Mg^{2+}·ATP for 30 min. The SDS-PAGE gel was evaluated via immunoblot using the G8 antibody pre- and post-incubation at different concentrations of Mg^{2+}·ATP. The shift to higher apparent molecular weights was only observed in fractions with Mg^{2+}·ATP (black arrow), indicating autophosphorylation. **(b)** Stabilization of GRK1 by ATP. The stability of GRK1 activity was assessed after incubation at 37 °C for up to 60 min in the presence or absence of 100 µM Mg^{2+}·ATP. **(c)** The effect of different Mg^{2+}·ATP concentrations on the activity of GRK1 after incubation at 37 °C for 30 min. Enzymatic activity increased with increasing Mg^{2+}·ATP concentrations.

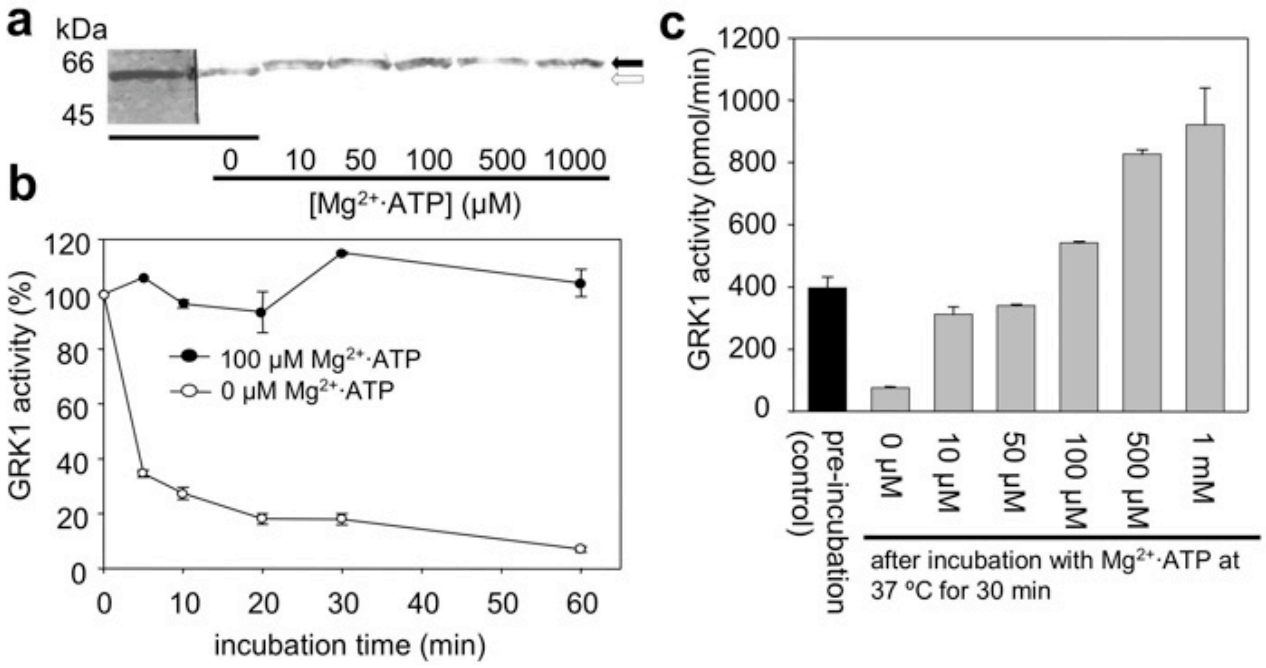

Figure S7. MS2 spectra of phosphopeptides from ATP-treated $GRK1_{535}$ and native bovine GRK1. (a) Ser21 is phosphorylated in $GRK1_{535}$-H_6 (Pool A, pre-treated with 4 mM ATP and 2 mM $MgCl_2$). **(b)** Ser488 and Thr489 are also phosphorylated in $GRK1_{535}$-H_6. **(c)** Ser5 is phosphorylated in GRK1 purified from bovine retinas.

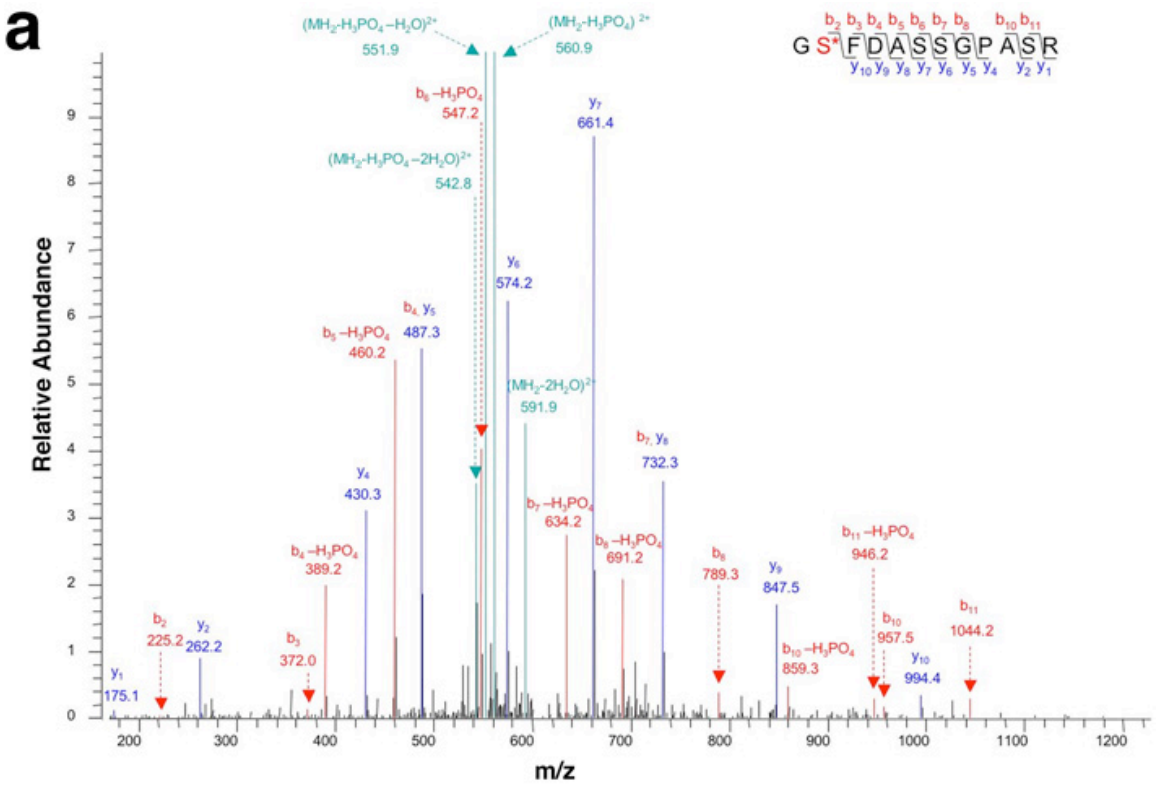

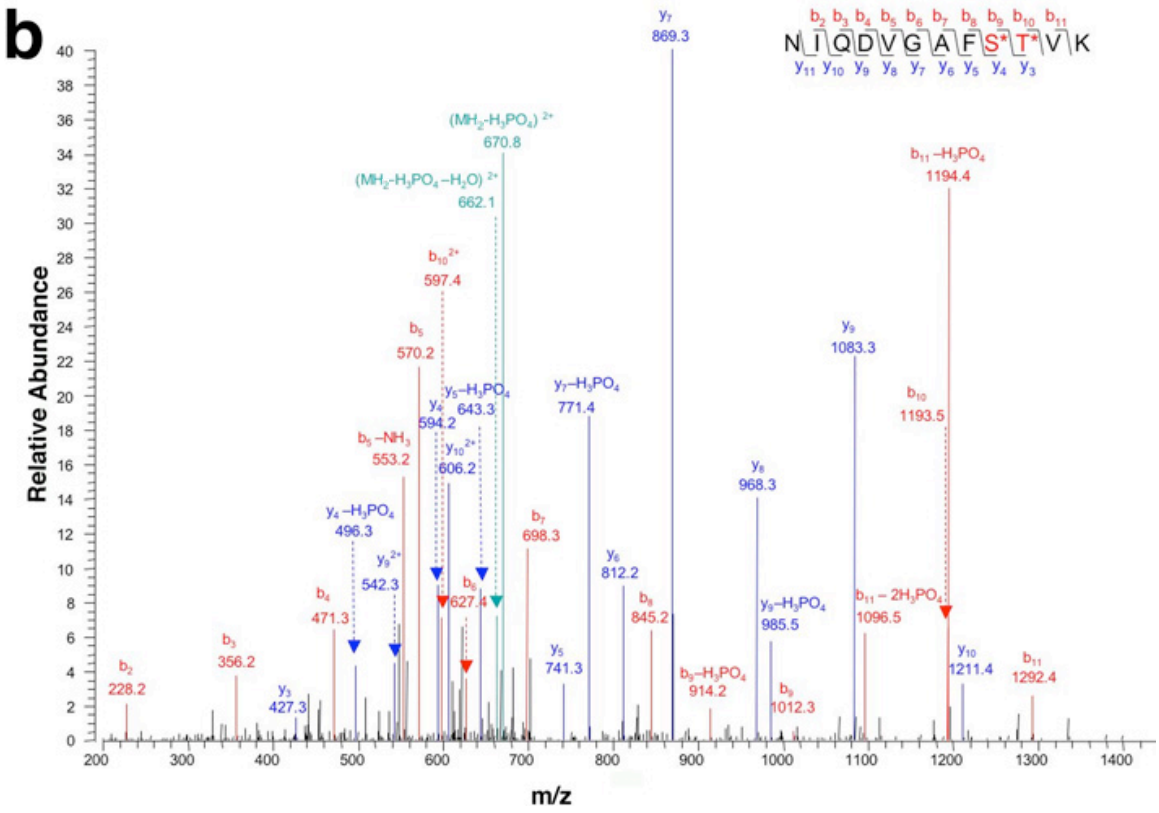
b
Relative Abundance
m/z
N I Q D V G A F S* T* V K
Acetyl-M D F G S* L E T V V A N S A F I A A R

Figure S8. Cation exchange chromatography of GRK1$_{535}$-His$_6$. GRK1$_{535}$-His$_6$ elutes in five peaks from a Source 15S column. Pool A elutes at NaCl concentration of 140-175 mM, Pool B as a doublet at 180-210 mM NaCl, and Pool C at ~220 mM. A fifth peak (Pool D) is aggregated. The inset shows that Pool A and C fractions migrate differently on a SDS-PAGE, even after pre-incubation with Mg^{2+}·ATP. Pool A corresponds to full-length acetylated GRK1$_{535}$-His$_6$ with potentially one or two phosphorylation sites (Supplementary Table S5).

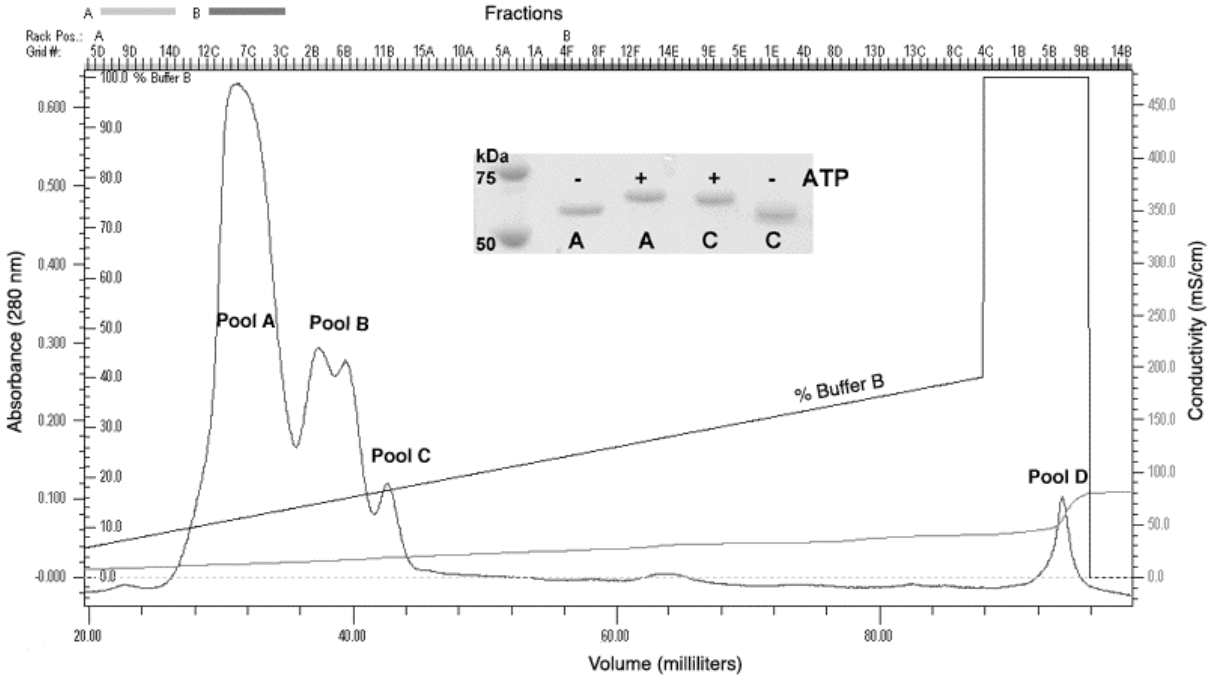

Figure S9. Binding of GRK1$_{535}$-His$_6$ to a recoverin affinity column. Equal amounts (50 μg) of Pool A, B and C samples (LOAD) were incubated with myr$^-$-recoverin coupled to Sepharose CL-4B beads. The bound protein was eluted (BOUND) with a buffer lacking $CaCl_2$. The unbound protein is in the flow-through (FREE). Compared with Pool A, Pool B displays reduced binding whereas Pool C has no detectable affinity for the column. The experiment was repeated twice, each with the binding reactions performed in triplicate, as shown.

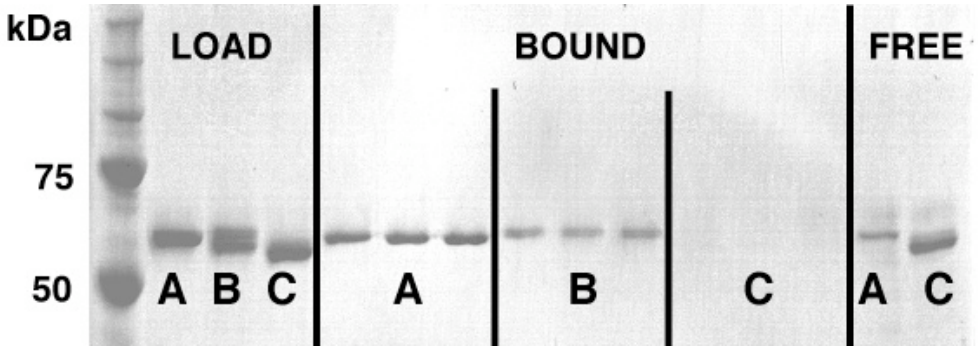

Figure S10. Recoverin column purification of native GRK1. Native GRK1 was eluted in one peak from CNBr-activated Sepharose CL-4B beads coupled to recoverin with modified ROS buffer with 5 mM EGTA as the final purification step. The eluted fractions with GRK1 activity were evaluated by SDS-PAGE and immunoblot as shown in the inset.

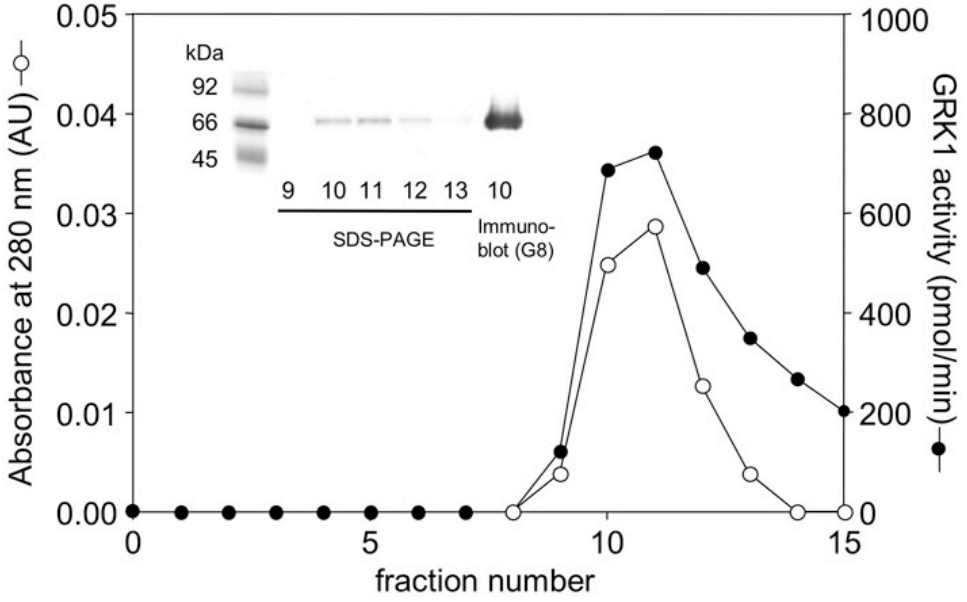

Figure S11. Six crystal forms of GRK1. (a) Crystals of GRK1·$(Mg^{2+})_2$·ATP (crystal form I) were grown at 4 ˚C to dimensions of 0.6 x 0.02 x 0.06 mm over the course of one week. (**b**) Crystal form II grew at 4 ˚C to similar dimensions. **(c)** Crystals of apo-GRK1 (crystal form III) grew at 4 ˚C to dimensions of 0.36 x 0.04 x 0.04 mm. These crystals took the longest to nucleate (~ 2 weeks). **(d)** Crystals of the GRK1·$(Mg^{2+})_2$·ADP complex (crystal form IV) were grown at 20 °C to dimensions of 0.2 x 0.12 x 0.08 mm. **(e)** Crystal form V grew at 4˚ C to dimensions of 0.2 x 0.05 x 0.02 mm. **(f)** Crystal form VI grew at 4˚ C to dimensions of 0.32 x 0.28 x 0.04 mm.

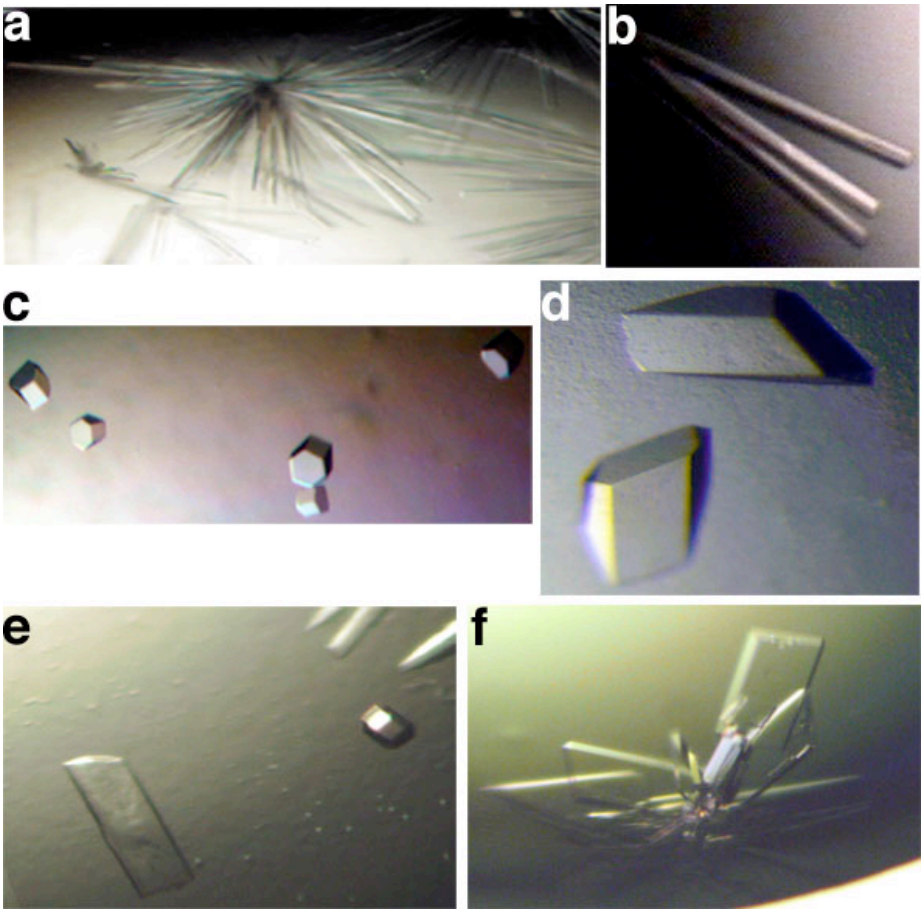

SUPPLEMENTARY REFERENCES

1. Chen, C. K., Inglese, J., Lefkowitz, R. J., and Hurley, J. B. (1995) *J Biol Chem* **270**(30), 18060-18066
2. Pronin, A. N., Loudon, R. P., and Benovic, J. L. (2002) *Methods Enzymol* **343**, 547-559
3. Lodowski, D. T., Tesmer, V. M., Benovic, J. L., and Tesmer, J. J. (2006) *J Biol Chem* **281**(24), 16785-16793